Supporting Information

Synthesis, structures and magnetic properties of a family of nitrate-bridged octanuclear [Na_2Ln_6] (Ln = Dy, Tb, Gd, Sm) complexes

Shi-Xiong She,[a] Yanmei Chen,[a] Mike J Zawortotko,[b] Wei Liu,[a] Yanyuan Cao,[a] Jian Wu[a] and Yahong Li[*a, c]

[a] *Key Laboratory of Organic Synthesis of Jiangsu Province, College of Chemistry, Chemical Engineering and Materials Science, Soochow University, Suzhou 215006, China. E-mail: liyahong@suda.edu.cn*

[b] *Department of Chemistry, University of South Florida, CHE205, 4202 East Fowler Avenue Tampa, FL 33620-5250, USA*

[c] *State Key Laboratory of Applied Organic Chemistry, Lanzhou University, Lanzhou, 730000, China*

Table S1 Data collection and processing parameters for complexes **1-4**

	1	**2**	**3**	**4**
Empirical formula	$C_{140}H_{165}Dy_6N_{13}Na_2O_{71}$	$C_{140}H_{165}N_{13}Na_2O_{71}Tb_6$	$C_{140}H_{161}Gd_6N_{13}Na_2O_{70}$	$C_{140}H_{165}N_{13}Na_2O_{72}Sm_6$
Formula weight	4186.82	4165.4	4135.32	4130.03
Temperature/K	293(2)	293(2)	293(2)	293(2)
Crystal system	monoclinic	monoclinic	monoclinic	monoclinic
Space group	*C*2/c	*C*2/c	*C*2/c	*C*2/c
a/Å	28.4980(18)	28.8424(5)	28.6753(15)	28.7428(17)
b/Å	19.3970(11)	19.6010(3)	19.3572(10)	19.4232(11)
c/Å	30.5590(18)	30.8266(5)	30.6841(16)	30.7742(18)
α/°	90.00	90.00	90.00	90.00
β/°	103.5140(11)	104.0500(10)	104.296(3)	104.145(3)
γ/°	90.00	90.00	90.00	90.00
Volume/Å^3	16424.6(17)	16906.1(5)	16504.5(15)	16659.6(17)
Z	4	4	4	4
ρ_{calc}mg/mm^3	1.693	1.653	1.726	1.668
m/mm^{-1}	2.807	2.579	2.485	2.186
F(000)	8832.0	8392.0	8576.0	8384.0
Crystal size/mm^3	0.21 × 0.16 × 0.12	0.23 × 0.15 × 0.14	0.24 × 0.16 × 0.13	0.2 × 0.14 × 0.1
ϴ range	3.5 to 56.74°	2.92 to 60.72°	2.94 to 50.18°	2.72 to 56.72°
Index ranges	$-30 \le h \le 38$ $-19 \le k \le 25$, $-40 \le l \le 40$	$-40 \le h \le 40$ $-27 \le k \le 27$ $-33 \le l \le 43$	$-34 \le h \le 33$ $-23 \le k \le 23$ $-36 \le l \le 36$	$-38 \le h \le 38$ $-25 \le k \le 25$ $-40 \le l \le 41$
Reflections collected	56274	90594	61981	79654
Independent reflections	20511[*R*(int) = 0.0376]	25263[*R*(int) = 0.0300]	14598[*R*(int) = 0.0543]	20625[*R*(int) = 0.0550]
Data/restraints/parameters	20511/237/1025	25263/256/1040	14598/227/1016	20625/255/1037
Goodness-of-fit on F^2	1.015	1.040	1.061	1.020
Final *R* indexes [$I>=2\sigma(I)$]	R_1 = 0.0312, wR_2 = 0.0708	R_1 = 0.0384, wR_2 = 0.1089	R_1 = 0.0511, wR_2 = 0.1532	R_1 = 0.0402, wR_2 = 0.0985
Final *R* indexes [all data]	R_1 = 0.0414, wR_2 = 0.0739	R_1 = 0.0552, wR_2 = 0.1180	R_1 = 0.0695, wR_2 = 0.1663	R_1 = 0.0624, wR_2 = 0.1063
Largest diff. peak/hole / e Å^{-3}	1.48/-1.02	2.06/-1.18	2.44/-1.33	1.28/-1.47

Table S2 Selected bond distances (Å) for complexes **1-4**

	1 (Ln=Dy)	**2(Ln=Tb)**	**3 (Ln=Gd)**	**4 (Ln=Sm)**
Ln1−O3	2.312(2)	2.316(3)	2.320(6)	2.348(3)
Ln1−O5	2.247(2)	2.251(3)	2.273(5)	2.290(3)
Ln1−O8	2.6838(2)	2.6961(2)	2.7044(4)	2.7091(3)
Ln1−O9	2.393(2)	2.416(2)	2.426(4)	2.444(3)
Ln1−O10	2.418(2)	2.447(3)	2.496(5)	2.515(3)
Ln1−O11	2.405(2)	2.414(3)	2.420(5)	2.445(3)
Ln1−O12	2.547(2)	2.559(3)	2.552(5)	2.565(3)
Ln1−O15	2.445(2)	2.465(3)	2.497(5)	2.519(3)
Ln1−N1	2.574(3)	2.597(3)	2.596(6)	2.601(4)
Ln1−N2	2.9130(16)	2.9356(17)	2.947(4)	2.951(2)
Ln2−O1	2.368(2)	2.386(2)	2.399(5)	2.421(3)
Ln2−O2^{1}	2.378(2)	2.387(2)	2.400(4)	2.400(3)
Ln2−O2	2.342(2)	2.353(2)	2.373(4)	2.413(3)
Ln2−O9	2.379(2)	2.389(2)	2.407(4)	2.431(3)
Ln2−O12	2.479(2)	2.493(2)	2.517(5)	2.520(3)
Ln2−O13	2.354(2)	2.363(3)	2.377(5)	2.408(3)
Ln2−O14	2.372(2)	2.385(2)	2.395(5)	2.417(3)
Ln2−O16	2.309(2)	2.324(2)	2.334(5)	2.352(3)
Ln3−O1	2.344(2)	2.359(2)	2.381(5)	2.408(3)
Ln3−O1^{1}	2.340(2)	2.351(2)	2.354(5)	2.379(3)
Ln3−O2	2.367(2)	2.380(2)	2.388(5)	2.408(3)
Ln3−O18	2.383(2)	2.407(3)	2.446(6)	2.475(4)
Ln3−O19^{1}	2.332(2)	2.345(3)	2.375(5)	2.401(3)
Ln3−O20	2.317(2)	2.324(3)	2.336(5)	2.347(3)
Ln3−O22	2.324(2)	2.332(3)	2.373(5)	2.387(3)
Ln3−O24^{1}	2.509(2)	2.533(3)	2.494(5)	2.494(3)

Table 3 Selected bond angles (º) for complexes **1**-**4**

			Ln=Dy	**Ln=Tb**	**Ln=Gd**	**Ln=Sm**
Atom	**Atom**	**Atom**	**Angle/°**	**Angle/°**	**Angle/°**	**Angle/°**
O3	Ln1	O8	67.23(6)	67.70(7)	67.26(13)	67.40(7)
O3	Ln1	O9	76.53(7)	76.76(9)	76.97(16)	77.30(10)
O3	Ln1	O10	142.53(9)	142.25(11)	141.45(19)	140.97(11)
O3	Ln1	O11	87.17(8)	86.75(10)	88.05(19)	88.11(11)
O3	Ln1	O12	118.66(7)	118.23(9)	119.43(18)	119.39(10)
O3	Ln1	O15	138.37(8)	138.98(9)	138.73(17)	138.73(10)
O3	Ln1	N1	68.59(8)	68.26(10)	68.15(19)	67.64(11)
O3	Ln1	N2	73.43(6)	73.98(7)	73.92(13)	74.16(8)
O5	Ln1	O3	96.01(8)	96.67(10)	96.3(2)	96.18(11)
O5	Ln1	O8	74.61(8)	74.94(9)	75.04(17)	75.08(11)
O5	Ln1	O9	124.43(8)	124.26(9)	123.94(15)	123.80(9)
O5	Ln1	O10	78.86(8)	78.80(10)	78.56(19)	78.32(11)
O5	Ln1	O11	137.59(8)	137.76(10)	137.50(18)	137.72(11)
O5	Ln1	O12	145.31(8)	145.09(10)	144.29(19)	144.42(10)
O5	Ln1	O15	75.52(8)	75.38(10)	74.85(18)	74.66(10)
O5	Ln1	N1	71.09(8)	70.93(10)	70.84(19)	71.05(11)
O5	Ln1	N2	98.78(9)	99.13(10)	98.90(19)	98.74(11)
O8	Ln1	N2	26.03(9)	26.17(10)	25.9(2)	25.75(11)
O9	Ln1	O8	51.43(8)	51.04(9)	50.71(16)	50.57(10)
O9	Ln1	O10	136.67(8)	136.51(10)	137.35(18)	137.63(11)
O9	Ln1	O11	97.51(8)	97.59(9)	98.27(16)	98.23(10)
O9	Ln1	O12	67.56(7)	67.85(8)	68.25(14)	68.17(9)
O9	Ln1	O15	75.58(7)	75.40(9)	75.56(16)	75.40(9)
O9	Ln1	N1	143.49(8)	143.66(10)	143.80(19)	143.63(10)
O9	Ln1	N2	25.86(8)	25.36(9)	25.29(18)	25.33(10)
O10	Ln1	O8	142.48(7)	142.69(8)	143.31(15)	143.35(9)
O10	Ln1	O12	74.25(7)	73.98(9)	74.05(18)	74.50(10)
O10	Ln1	O15	76.79(8)	76.68(10)	77.31(18)	77.62(11)
O10	Ln1	N1	74.74(9)	74.98(11)	74.2(2)	74.16(12)
O10	Ln1	N2	143.96(7)	143.74(9)	144.54(15)	144.76(9)
O11	Ln1	O8	142.50(7)	142.27(9)	142.85(16)	142.73(10)
O11	Ln1	O10	73.60(8)	73.48(11)	72.4(2)	72.49(11)
O11	Ln1	O12	52.45(8)	51.98(9)	52.09(17)	51.80(10)
O11	Ln1	O15	126.62(8)	126.28(9)	125.90(18)	125.91(10)
O11	Ln1	N1	70.93(8)	71.49(10)	71.8(2)	71.96(11)
O11	Ln1	N2	122.36(8)	122.00(10)	122.70(19)	122.68(11)
O12	Ln1	O8	115.98(8)	116.02(9)	115.99(16)	115.88(10)
O12	Ln1	N1	120.79(8)	120.89(9)	121.35(18)	121.37(10)
O12	Ln1	N2	90.53(9)	90.39(9)	90.62(19)	90.65(11)
O15	Ln1	O8	71.25(5)	71.40(6)	71.53(12)	71.37(7)
O15	Ln1	O12	77.30(7)	77.39(8)	77.12(16)	77.41(9)

O15	Ln1	N1	139.42(8)	139.30(10)	138.81(19)	139.05(11)
O15	Ln1	N2	67.96(5)	67.94(6)	68.06(11)	67.91(7)
N1	Ln1	O8	119.43(8)	119.25(9)	119.05(18)	118.95(11)
N1	Ln1	N2	139.05(8)	139.11(9)	138.94(18)	138.68(10)
O1	Ln2	O2[1]	68.95(7)	68.79(8)	68.68(15)	68.71(9)
O1	Ln2	O9	143.29(7)	142.89(8)	142.62(14)	142.33(9)
O1	Ln2	O12	144.54(7)	144.62(8)	145.39(15)	145.80(9)
O1	Ln2	O14	123.82(7)	123.56(8)	123.33(16)	123.17(9)
O2	Ln2	O1	69.65(7)	69.27(8)	68.88(16)	68.72(9)
O2	Ln2	O2[1]	71.02(8)	70.42(9)	70.30(18)	70.11(10)
O2	Ln2	O9	89.89(7)	89.50(8)	75.56(15)	88.93(9)
O2[1]	Ln2	O9	75.76(7)	75.61(8)	89.41(14)	75.39(9)
O2	Ln2	O12	139.90(7)	140.28(8)	130.68(16)	139.83(9)
O2[1]	Ln2	O12	130.32(7)	130.57(8)	139.83(16)	130.35(9)
O2	Ln2	O13	147.00(7)	146.74(9)	147.20(16)	147.19(9)
O2	Ln2	O14	71.86(7)	72.31(8)	72.22(16)	72.07(9)
O9	Ln2	O12	68.91(7)	69.37(8)	69.13(15)	69.10(9)
O13	Ln2	O1	90.15(8)	90.47(9)	91.62(17)	92.25(10)
O13	Ln2	O2[1]	77.53(8)	77.82(9)	78.19(16)	78.22(9)
O13	Ln2	O9	91.89(8)	92.06(10)	91.45(18)	91.31(10)
O13	Ln2	O12	70.10(7)	69.91(9)	69.65(16)	69.28(10)
O13	Ln2	O14	139.79(8)	139.62(9)	139.02(17)	138.91(10)
O14	Ln2	O2[1]	131.28(7)	131.37(8)	131.14(15)	130.76(9)
O14	Ln2	O9	73.74(7)	73.96(8)	73.84(16)	73.53(9)
O14	Ln2	O12	69.69(8)	69.71(9)	69.37(16)	69.64(9)
O16	Ln2	O1	74.51(7)	74.58(9)	74.79(16)	74.68(10)
O16	Ln2	O2	97.85(8)	98.26(9)	97.90(17)	97.47(9)
O16	Ln2	O2[1]	143.42(7)	143.34(8)	143.45(17)	143.39(10)
O16	Ln2	O9	140.33(7)	140.52(9)	140.33(17)	140.33(9)
O16	Ln2	O12	80.84(8)	80.68(9)	80.91(17)	81.62(10)
O16	Ln2	O13	101.57(8)	101.42(10)	102.13(18)	103.03(11)
O16	Ln2	O14	71.98(8)	71.81(9)	71.56(17)	71.46(10)
O1[1]	Ln3	O1	69.74(9)	69.54(10)	69.24(18)	69.10(11)
O1	Ln3	O2	69.63(7)	69.29(8)	68.93(15)	68.79(9)
O1[1]	Ln3	O2	69.59(7)	69.48(8)	69.61(16)	69.48(9)
O1[1]	Ln3	O18	73.38(8)	100.01(10)	99.04(19)	72.15(11)
O1	Ln3	O18	99.78(8)	73.40(9)	72.84(18)	98.99(11)
O1	Ln3	O24[1]	150.88(7)	151.35(9)	152.23(16)	152.24(10)
O1[1]	Ln3	O24[1]	125.24(8)	125.63(9)	125.54(17)	125.66(10)
O2	Ln3	O18	142.89(7)	142.80(9)	142.42(18)	141.59(10)
O2	Ln3	O24[1]	136.66(8)	136.36(9)	135.85(17)	136.01(10)
O18	Ln3	O24[1]	66.65(8)	67.10(10)	68.4(2)	68.82(11)
O19[1]	Ln3	O1	141.44(7)	141.29(9)	140.92(17)	140.57(10)
O19[1]	Ln3	O1[1]	78.30(8)	78.73(9)	79.23(17)	79.07(10)

O19[1]	Ln3	O2	79.53(8)	79.35(9)	78.99(16)	78.82(10)
O19[1]	Ln3	O18	90.91(9)	91.30(12)	92.9(2)	92.53(13)
O19[1]	Ln3	O24[1]	66.85(8)	66.71(9)	66.32(18)	66.66(11)
O20	Ln3	O1	74.66(8)	74.32(9)	74.73(18)	74.50(10)
O20	Ln3	O1[1]	130.99(8)	130.19(9)	131.47(18)	131.49(10)
O20	Ln3	O2	126.40(8)	126.40(9)	124.89(17)	124.37(11)
O20	Ln3	O18	80.88(8)	80.56(11)	82.1(2)	83.34(13)
O20	Ln3	O19[1]	143.88(8)	144.35(10)	144.09(19)	144.62(11)
O20	Ln3	O22	73.03(8)	73.64(10)	73.43(18)	72.79(11)
O20	Ln3	O24[1]	77.69(8)	78.24(10)	78.93(19)	79.23(11)
O22	Ln3	O1[1]	147.86(7)	147.70(9)	146.14(16)	146.16(10)
O22	Ln3	O1	104.48(8)	104.12(9)	104.23(17)	103.80(10)
O22	Ln3	O2	78.72(7)	78.61(8)	77.02(16)	77.09(9)
O22	Ln3	O18	137.73(8)	137.96(10)	140.03(19)	140.80(11)
O22	Ln3	O19[1]	91.13(8)	90.87(10)	89.13(18)	89.72(10)
O22	Ln3	O24[1]	75.55(8)	75.43(10)	76.05(19)	76.35(11)
Ln3	O1	Ln2	107.18(8)	107.37(9)	107.74(18)	107.89(10)
Ln3[1]	O1	Ln2	108.63(8)	108.39(9)	108.16(18)	107.86(10)
Ln3[1]	O1	Ln3	106.23(8)	106.48(9)	106.79(17)	106.97(10)
Ln2	O2	Ln2[1]	105.17(8)	105.67(8)	105.72(17)	105.87(9)
Ln2	O2	Ln3	107.26(8)	107.74(9)	108.39(17)	108.58(10)
Ln3	O2	Ln2[1]	107.37(8)	107.42(9)	107.05(17)	107.17(10)
Ln1[1]	O8	Ln1	174.05(12)	174.57(14)	175.2(3)	175.41(17)
Ln2	O9	Ln1	115.86(8)	115.30(9)	115.04(16)	114.62(10)
Ln2	O12	Ln1	107.17(8)	106.93(9)	107.07(16)	107.57(10)
Ln1[1]	N2	Ln1	133.88(15)	133.09(15)	133.0(3)	133.09(18)

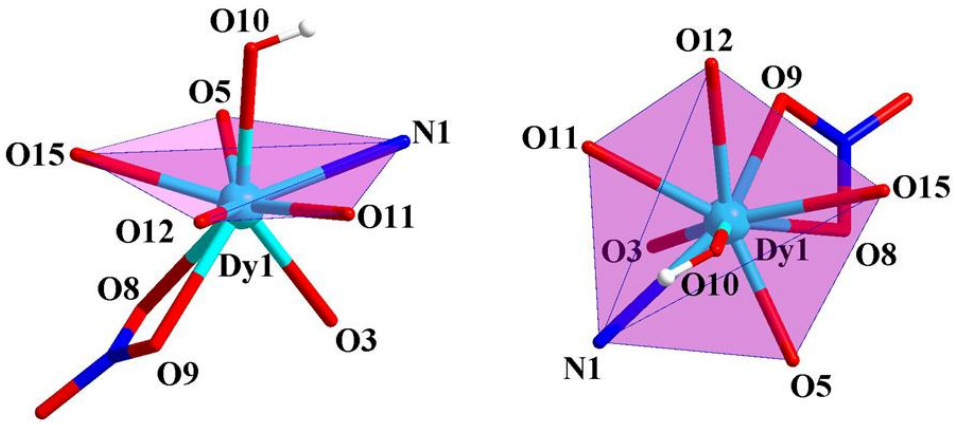

Figure S1. A) Side view and B) top view of the hula hoop-like coordination environment of the Dy1 ion in complex **1.**

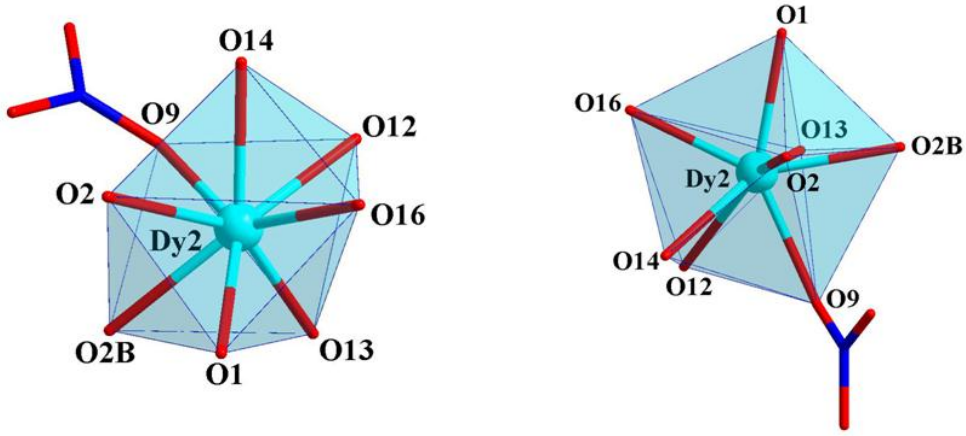

Figure S2. A) Side view and B) top view of the square-antiprismatic coordination environment of the Dy2 ion in complex **1**.

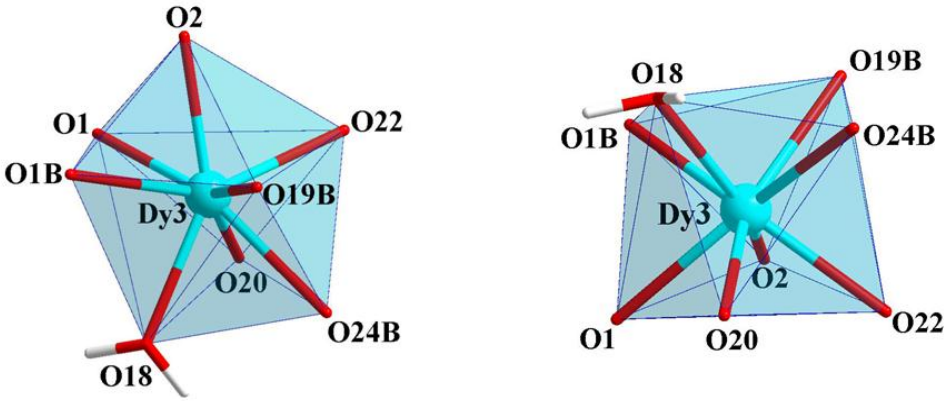

Figure S3. A) Side view and B) top view of the square-antiprismatic coordination environment of the Dy3 ion in complex **1**.

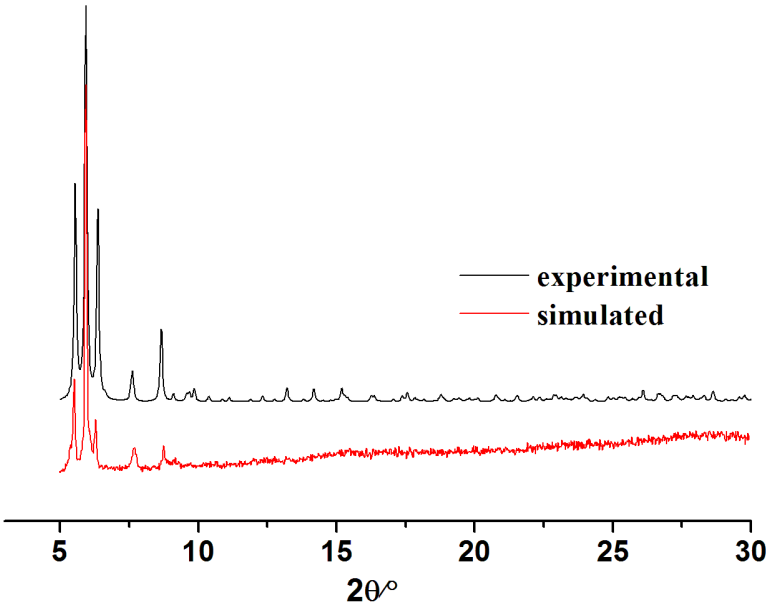

Figure S4. The simulated and experimental PXRD pattern of complex **1**

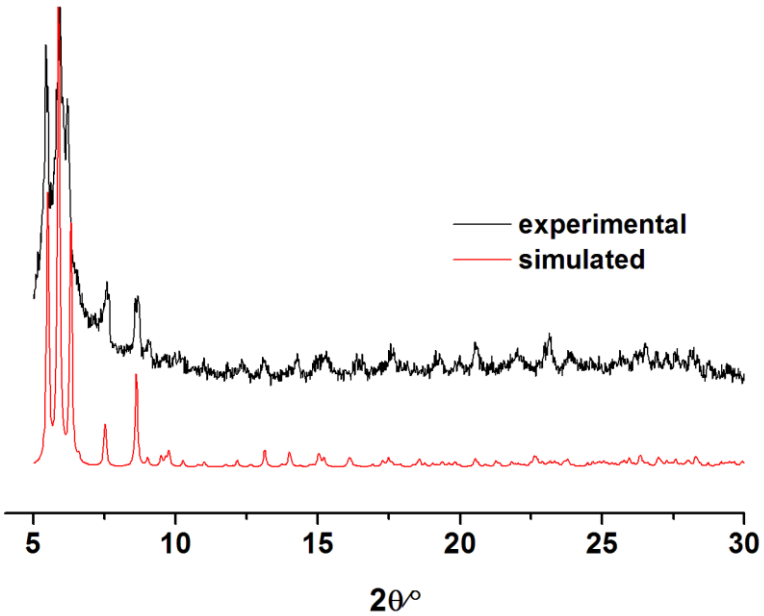

Figure S5. The simulated and experimental PXRD pattern of complex **2**

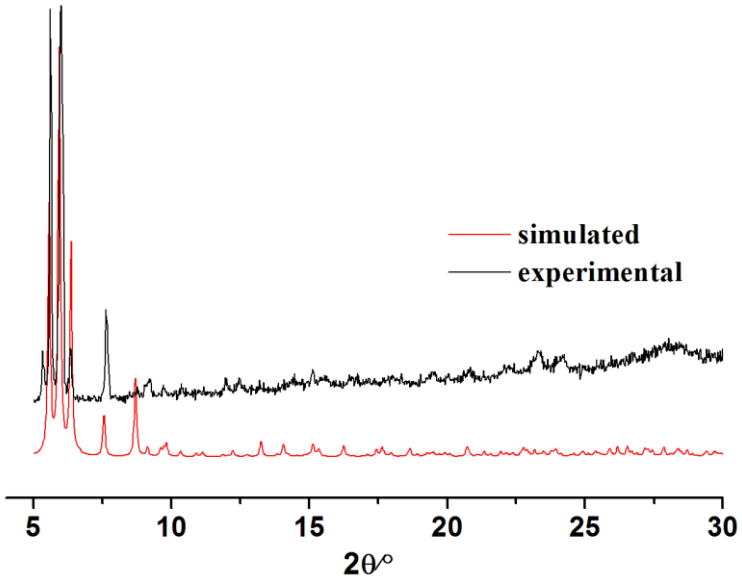

Figure S6. The simulated and experimental PXRD pattern of complex **3**

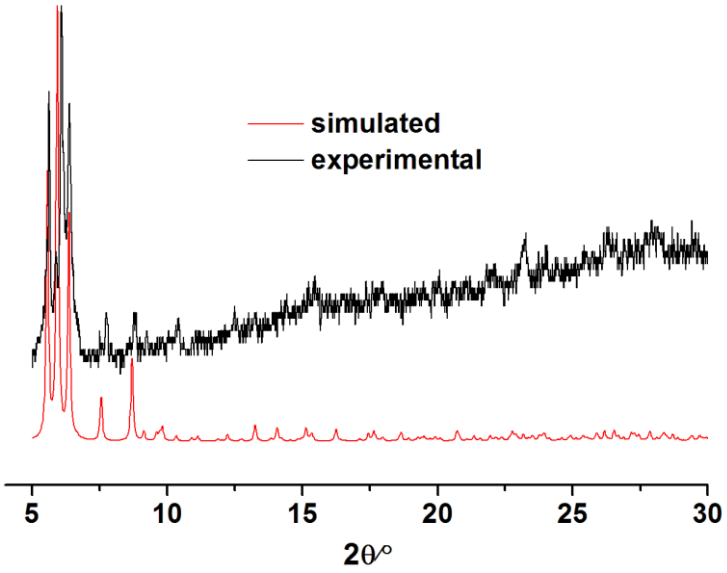

Figure S7. The simulated and experimental PXRD pattern of complex **4**

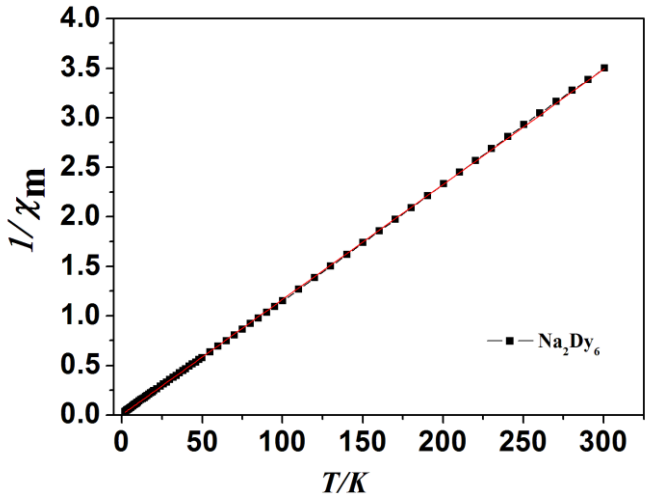

Figure S8. The plot of $1/\chi_M$ versus T for compound **1** and the linear fit of Curie-Weiss law at 1000 Oe field.

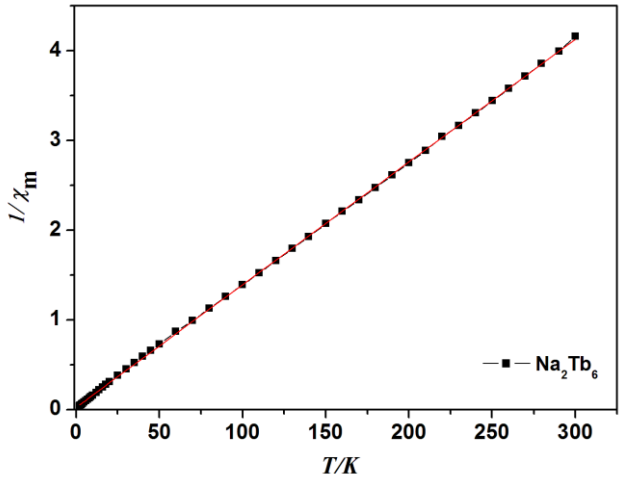

Figure S9. The plot of $1/\chi_M$ versus T for compound **2** and the linear fit of Curie-Weiss law at 1000 Oe field.

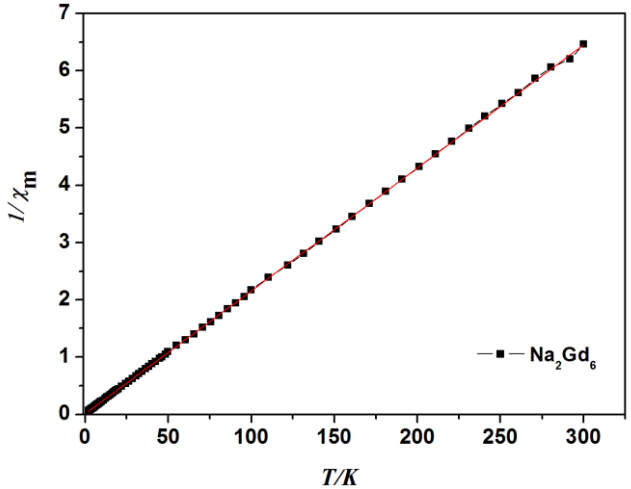

Figure S10. The plot of $1/\chi_M$ versus T for compound **3** and the linear fit of Curie-Weiss

law at 1000 Oe field.

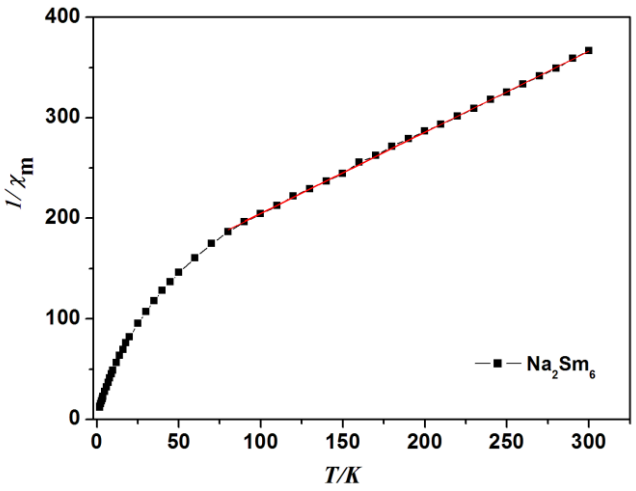

Figure S11. The plot of $1/\chi_M$ versus T for compound **4** and the linear fit of Curie-Weiss law at 1000 Oe field.

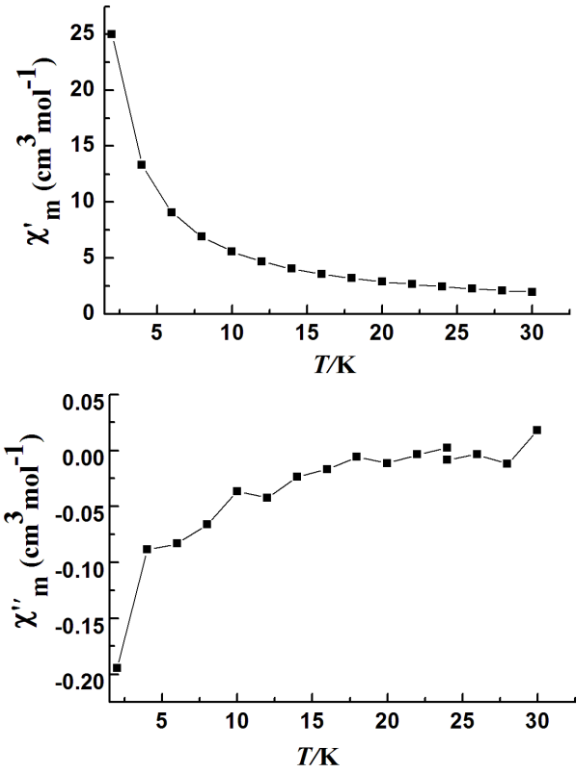

Figure S12. Temperature dependence of the in-phase (top) and out-of-phase (bottom) ac susceptibility for **2** under zero dc field at 1000 Hz.

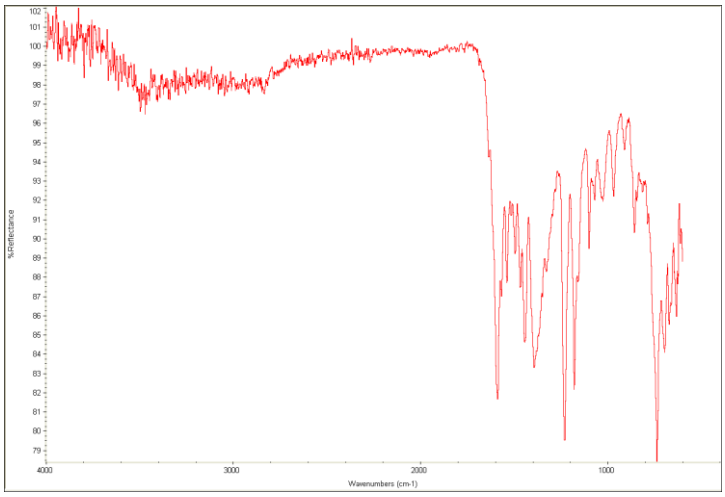

Fig. S13 The IR spectrum of complex **1**

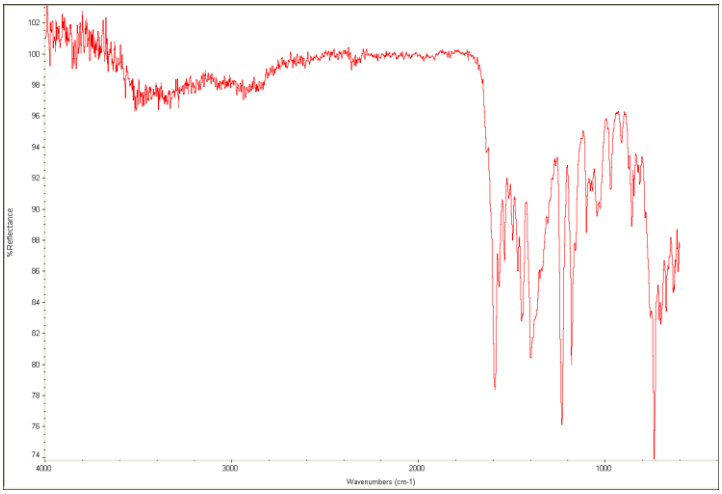

Fig. S14 The IR spectrum of complex **2**

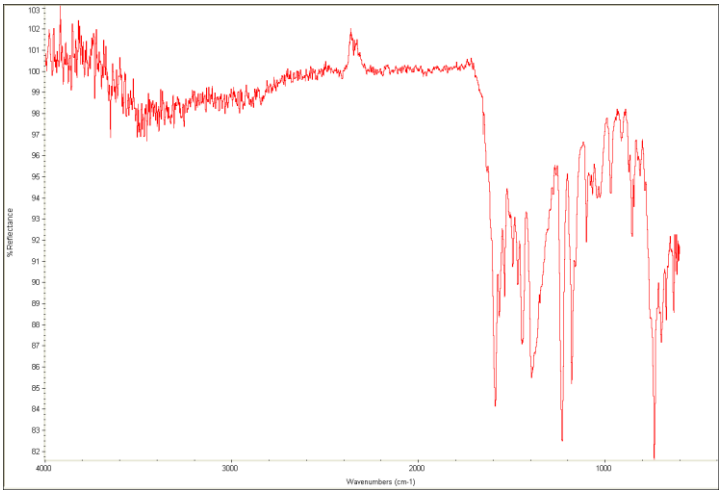

Fig. S15 The IR spectrum of complex **3**

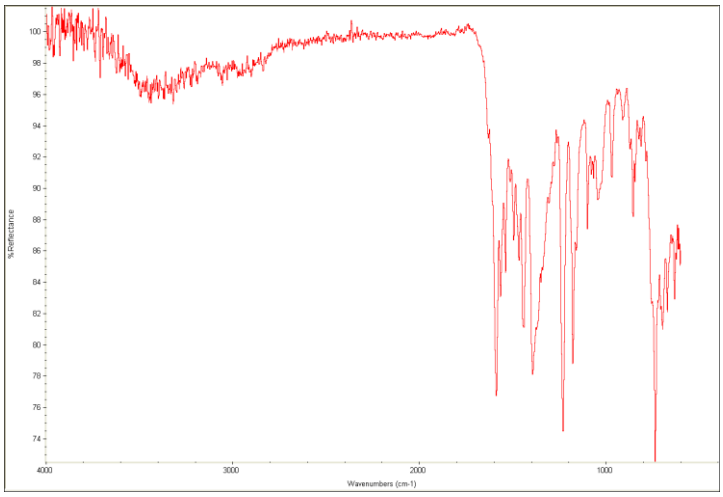

Fig. S16 The IR spectrum of complex **4**